MODELLING OF A NON LINEAR SOLENOID ACTUATOR FOR OPERATION AS A PROPORTIONAL ACTUATOR.

M. F. Rahman, N. C. Cheung & K. W. Lim
University of New South Wales
Sydney 2052, Australia

1. Abstract

This paper describes the modelling of a non linear solenoid with a view to convert an on/off solenoid into a proportional actuator. It investigates the magnetic characteristics of a solenoid and proposes an efficient dynamic model for the device. The model exploits the fact that the magnetic characteristics of a solenoid contain a linear and a saturated region. A linear magnetic circuit is used to describe the linear region. For the saturated region, a second order function is used to approximate the flux-current characteristics, and a reciprocal function is used to approximate the flux-position characteristics. This modelling method leads to some simplification of analysis and implementation of the proportional actuator on a digital signal processor. It is further validated by comparing the solenoid's simulated dynamic response with its actual dynamic response.

2. Introduction

SOLENOIDS are widely used as switching actuators. They are simple in construction, rugged, and relatively cheap to produce. For these reasons they can be found in many industrial and domestic apparatus in which limited stroke, on/off mechanical movements are required. Solenoids are normally used in the form of electrical contactors in relays, in the form of throttling devices in fluid/gas valves, and linear/rotary motional devices which operate in one of two positions - open and close. On the other hand, conventional proportional actuators are high precision, limited travel motional devices, driven by step motors, moving coil actuator, or other motors with a linear control characteristic. Such proportional actuators are more complex in construction, contain delicate moving and sensing elements, and is expensive to produce and maintain. Examples of applications include fluid flow controller in hydraulic servo systems, grasping motions in robot fingers, robot joints, positioning systems, machine tool drives, etc.

The paper describes part of a project which aims to convert a cheap on/off solenoid into a proportional actuator by the use of intelligent control [1,2]. The project is motivated by three considerations. Firstly, solenoids have a small and compact size, and the production cost is much lower than traditional proportional actuators. Secondly, solenoids have simple constructions, they are robust and maintenance free. Therefore higher reliability can be obtained. Finally, solenoids can easily incorporated into systems design due to its compact size and robust construction. However, to convert a switching solenoid into a proportional actuator is straight forward task because of the highly nonlinear magnetic characteristic of the device. It is also a variable reluctance device with its force derived from the change in its magnetic circuit. Though there has been a renewed interest in variable reluctance motors [3,4,5,6], there is little literature which deals with the modelling and precise control of solenoids.

In this paper, the control characteristics of the solenoid is investigated and an efficient model for the solenoid is proposed. The model has been subsequently used effectively in the analysis and implementation of a proportional solenoid [2]. The paper first examines the control dynamics and magnetic characteristics of a solenoid. A method for modelling a solenoid, including its non linear magnetic characteristics, is then proposed. This model can be used to predict the electrical and mechanical dynamic response of a solenoid. Finally, results of the modelling exercise is tested on a typical industrial solenoid and validated by comparing the dynamic simulation of the device with experimental measurements.

3. Control and Magnetic Characteristics of the Linear Travel Solenoid

Figure 1 shows the construction of a linear and limited travel solenoid. The solenoid's plunger retracts inward when the coil is energised, and extends outward by releasing the stored energy from the spring. Total travel of the plunger is very short: in most cases, it is limited to about one centimetre. In order to achieve a high force to size ratio, most solenoids operate well into the non linear magnetic saturation region.

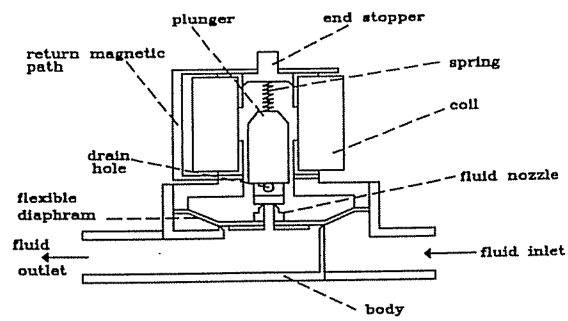

Figure 1. A two stage solenoid valve.

(1) Dynamic characteristics of a solenoid

The solenoid is operated normally by applying a voltage to its coil, the voltage equation being expressed as:

$$V = Ri + \frac{d\lambda}{dt} \tag{1}$$

where V is the terminal voltage and R is the resistance of coil. The flux linkage λ, is dependent on the coil current i, and the air gap distance x. Therefore the voltage equation can be rewritten as:

$$V = Ri + (L_e + \frac{\partial\lambda(x,i)}{\partial i})\cdot\frac{di}{dt} + \frac{\partial\lambda(x,i)}{\partial x}\cdot\frac{dx}{dt} \quad (2)$$

where L_e is the inductance of the external circuit. Of the three terms in the equation (2), the first term is the resistive voltage drop, the second term is the inductive voltage due to change of current. The third term is known as a motional e.m.f. which is caused by the motion of the plunger. Equation (2) can only be solved if the magnetic characteristics of the solenoid are known.

The motion of the solenoid's plunger can be represented by a mass spring system:

$$m_p\ddot{x} = F_{mag} - K_s x - m_p g \quad (3)$$

where m_p is the mass of the plunger, K_s is the spring constant, g is the gravitational constant, and F_{mag} is the force produced by magnetic field when the coil is energised. F_{mag} can be calculated from the co-energy W' of the magnetic circuit. The co-energy can be obtained from the integration of flux linkage λ against current i:

$$F_{mag} = \frac{\partial W'(x,i)}{\partial x} \quad (4)$$

$$W'(x,i) = \int_0^i \lambda(x,i)\cdot di \quad (5)$$

Since the variables i and x are fully independent and separable in relation to $\lambda(x,i)$, it is permissible to differentiate under the integral sign. Equation 4 and 5 become:

$$F_{mag} = \int_0^i \left.\frac{\partial\lambda(x,i)}{\partial x}\right|_{i=const}\cdot di \quad (6)$$

For the instantaneous value of F_{mag}, when x does not change during a short period of time, equation (6) can be written as:

$$F_{mag} = \frac{\partial\lambda(x,i)}{\partial x}\cdot i \quad (7)$$

From equations (2), (3), and (7) we can write the following set of nonlinear state equations (8 - 10) for the solenoid

$$\frac{dx}{dt} = v \quad (8)$$

$$\frac{dv}{dt} = (\frac{\partial\lambda(x,i)}{\partial x}\cdot i - K_s x - m_p g)\cdot\frac{1}{m_p} \quad (9)$$

$$\frac{di}{dt} = (V - Ri - \frac{\partial\lambda(x,i)}{\partial x}\cdot\frac{dx}{dt})\cdot\frac{1}{L_e + \frac{\partial\lambda(x,i)}{\partial i}} \quad (10)$$

In equations (8) to (10), $\partial\lambda/\partial x$ and $\partial\lambda/\partial i$ are obtained from a model of the magnetic characteristics. A parsimonious model of these characteristics is the key to the usefulness of these equations.

(2) Magnetic Characteristics of the Solenoid

The flux-current-position relation forms the basic characteristic of a solenoid. Since the solenoid operates well into the magnetic saturation region, its characteristics cannot be represented by simple linear equations. Figure 2 is a typical flux-current plot of a solenoid, with displacement x as a parameter. The curves show that flux linkage versus current is initially a linear relation. As the flux density increases, the curves become non linear. Also, different air gap positions have different degrees of non linearity.

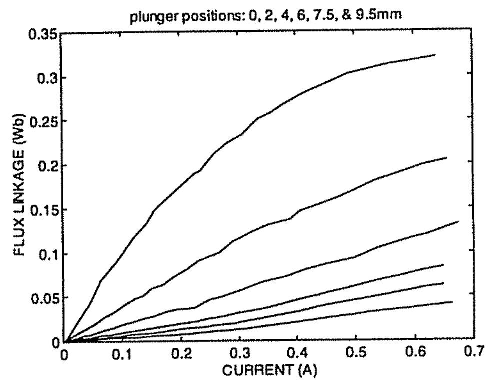

Figure 2. Measurements of flux linkage versus current at different positions.

Several curve fitting techniques are available for describing the magnetic characteristics of a variable reluctance machine [7]. However, they are either too complicated to implement in real time [8,9,10], or not sufficiently accurate for proportional solenoids. The curve fitting technique in [11] provides a balance between modelling accuracy and computation efficiency for a switched reluctance motor, but a different modelling description is required for the solenoid. All these methods are for variable reluctance motors only. Solenoids have a different magnetic structure.

In this paper, we propose to model the magnetic characteristics of a solenoid by dividing its operation into linear and saturated regions. A simple relation based on linear magnetic principles is used in the linear model. This is described first. For the saturated region, a parabolic curve approximation is used for the flux linkage versus current curves; and an inverse function approximation is used for the flux linkage versus position curves. This is described next. The proposed model provides a good balance between accuracy and computational efficiency.

(3) The linear Region

A description of the linear region can be obtained by using standard electromagnetic principles based on linear magnetic circuit. Consider a solenoid which operates within its linear region, and has the following parameters:

Equivalent cross sectional area for iron core and air gap:			A
Effective core length:	l	Air gap length:	x
No. of turns of coil:	N	Current through coil:	i
Permeability of free space:	μ_0	Relative permeability:	μ_r
Magnetic flux:	Φ		

$$Ni = \frac{l\Phi}{\mu_0\mu_r A} + \frac{x\Phi}{\mu_0 A} \quad (11)$$

The solenoid can be viewed as a variable reluctance magnetic circuit, with an mmf equation as in equation (11). It contains two terms; the first term describes the mmf drop due to the iron core, and the second term is the mmf drop due to the air gap. μ_r is treated as constant, since it operates below the saturation region. By substituting $\lambda = N\Phi$, equation (10) can be rearranged as:

$$\lambda(x,i) = \frac{\mu_0 A N^2 i}{\frac{l}{\mu_r} + x} \qquad (12)$$

By introducing two constant terms, K_a and K_b, equation (12) can be simplified as:

$$\lambda(x,i) = \frac{K_a}{K_b + x} \cdot i \qquad (13)$$

K_b is roughly constant, in spite of the fact that it changes with the plunger position. This is because K_b is much smaller than x for most of the time, and has little effect on the overall equation, except when x is close to zero. When x is very close to zero, the percentage of variation of K_b is very small and may be neglected.

Since leakage flux exists in solenoid, and a proportional amount of current is being used up to produce this leakage flux, equation (13) has to be compensated by *offset1* as shown in equation (14):

$$\lambda(x,i) = \left(\frac{K_a}{K_b + x} - \mathit{offset}1\right) \cdot i \qquad (14)$$

K_a, K_b, and *offset1* determines the linear portion of magnetic characteristics; these parameters are obtained by curve fitting equation (14) to the measured values of flux linkage versus position at $i=i_s$, by using a standard mathematical software package.

(4) Flux linkage versus current

Equation (14) is the general equation for describing the magnetic behaviour of a variable reluctance solenoid in the linear region. For the non linear region, the non linear plots are approximated by parabolic curves as shown in figure 3. The parabolic curve has a curvature of K_p with an origin point of $O(i_o,\lambda_o)$. It is represented by equation (15).

$$(\lambda_p - \lambda_0)^2 = 4K_p(i_p - i_0) \qquad (15)$$

In figure 3, λ_s is the flux saturation boundary, above which saturation will occur, $P(i_p,\lambda_p)$ is a point along the flux-current curve with position equal to x. L_x is the gradient of the linear part of the flux-current plot, and is obtained by:

$$L_x = \frac{\lambda}{i} = \frac{K_a}{K_b + x} - \mathit{offset}1 \qquad (16)$$

The saturation current i_s, can be obtained from the gradient L_x by:

$$i_s = \frac{\lambda_s}{L_x} \qquad (17)$$

In order to have a smooth transition between the linear and the non linear region, the gradient of the parabolic curve at point $S(i_s,\lambda_s)$ must be equal to the gradient in the linear region. Using this rule, i_o and λ_o can be found:

$$i_0 = i_s - \frac{K_p}{L_x^2} \qquad (18)$$

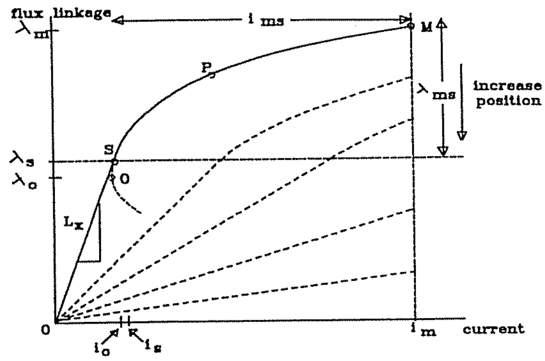

Figure 3. Curve fitting the flux-current characteristic of a solenoid by linear and parabolic approximation.

$$\lambda_0 = \lambda_s - \frac{2K_p}{L_x} \qquad (19)$$

The curvature of the curve is set so that the locus of the parabola will intersect point $M(i_m,\lambda_m)$:

$$K_p = \frac{\lambda_{ms}^2}{4\left(i_{ms} - \frac{\lambda_{ms}}{\lambda_m}\right)} \qquad (20)$$

where $\lambda_{ms} = \lambda_m - \lambda_s$; $i_{ms} = i_m - i_s$

This method constructs a parabolic curve based on two coordinates, $M(i_m,\lambda_m)$ and $S(i_s,\lambda_s)$ only. Since λ_s and i_m are predetermined values, therefore only i_s and λ_m needs to be determined. i_s can be obtained from equation (15), whereas λ_m can be obtained from a simple look up table of flux against position at i_m. Alternatively, λ_m can be calculated from the following equation:

$$\lambda_m = \frac{K_c}{K_d} - \mathit{offset}2 \qquad (21)$$

K_c, K_d, and *offset2* are found by curve fitting equation (21) to the flux linkage against position curve when $i=i_m$.

With this approach, flux linkage against current relation can be calculated by the following parameters with equations (16)-(21): K_a, K_b, K_c, K_d, λ_s, i_m, *offset1*, and *offset2*.

(5) Flux linkage versus position

Figure 4 is a typical flux linkage against position characteristic of a solenoid for a specified current. The curve in the linear region can be represented by equation (13). For the saturated region, the curve can be approximated by an inverse function. The function has the following form:

$$\lambda_p = \frac{K_1}{K_2 + x_p} - K_3 \qquad (22)$$

To have the above function pass through point $M(0,\lambda_m)$, K_1, K_2, and K_3 are specified as follows:

$$K_1 = K \cdot S_c \cdot \lambda_m \, ; \; K_2 = K \, ; \; K_3 = (S_c - 1) \cdot \lambda_m \qquad (23)$$

The value of K and S_c are selected so that the curve of described by equation (22) passes through point S and S_δ. By using the equation in the linear region, x_s can be obtained:

$$x_s = \frac{K_a}{offset1 + \frac{\lambda_s}{i}} - K_b \qquad (24)$$

Point $S_\delta(x_{s\delta}, \lambda_{s\delta})$ lies to the left and very close to point $S(x_s, \lambda_s)$. It is defined by the following relations:

$$x_{s\delta} = x_s - \delta \qquad (25)$$

$$\lambda_{s\delta} = \left(\frac{K_a}{K_b + x_{s\delta}} - offset1\right) \cdot i \qquad (26)$$

From equations (22) and (23), the following equations can be formed:

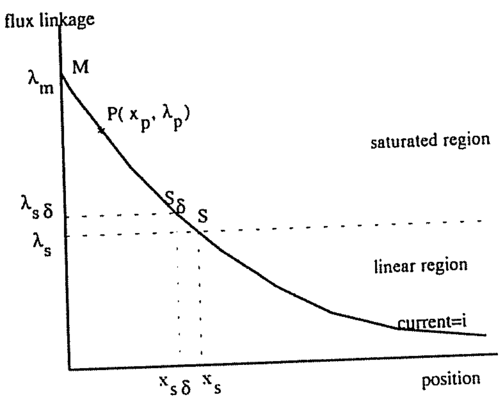

Figure 4. Curve fitting the flux-position characteristic of a solenoid by inverse functions approximation.

$$\lambda_s = \frac{K \cdot S_c \cdot \lambda_m}{K + x_s} - (S_s - 1)\lambda_m \qquad (27)$$

$$\lambda_{s\delta} = \frac{K \cdot S_c \cdot \lambda_m}{K + x_{s\delta}} - (S_c - 1)\lambda_m \qquad (28)$$

Once λ_m is obtained, the above two equations are used to solve K and S_c. K and S_c can be calculated as follows:

$$S_c = \frac{ac - c}{\frac{ac}{b} - 1} \qquad K = x_s \cdot \frac{S - b}{b}$$

$$\text{where} \quad a = \frac{x_s}{x_{s\delta}}; \quad b = 1 - \frac{\lambda_s}{\lambda_m} \quad ; \quad c = 1 - \frac{\lambda_{s\delta}}{\lambda_m} \qquad (29)$$

This method constructs a *1/x* function curve based on points M, S and S_δ only. λ_m can be obtained from a table of flux linkage against current when position $x=0$. Alternatively, λ_m can be calculated from the parabolic curve as described in the previous section. In this case, K_p, λ_o, and i_o at $x=0$ should be predetermined to enable faster calculation. With this approach, flux linkage versus position can be calculated by K_a, K_b, *offset1*, and λ_s by using equations (22)-(26) and (29).

The proposed modelling method exploits the fact that the magnetic circuit of a solenoid contains two operating regions: linear and saturated. For each operating region, the magnetic characteristic is described by a lowest order approximation function just sufficient for the required accuracy. In this way a model with the least complex describing functions is constructed. This model is computationally efficient, and is therefore very suitable for real-time computation of the solenoid's magnetic characteristics. For the same accuracy, there are other higher order and more general approximation methods available (eg. third order bi-cubic spline, sine-cosine description), but they require more complex calculations, and are less suitable for real time applications.

4. Measurement of Magnetic Characteristics

An industrial solenoid of the type shown in figure 1 was used for the modelling. The rating of the solenoid is 24 V and 0.6 A. The first step was to determine the magnetic characteristics accurately. A sinusoidal voltage was applied to the coil of the solenoid for each position of its plunger and the hysteresis loops traversed by the solenoid were computed. Knowing the number of turns of the coil and by joining the vertices of the hysteresis loops, flux linkage vs position and current characteristics curves were obtained.

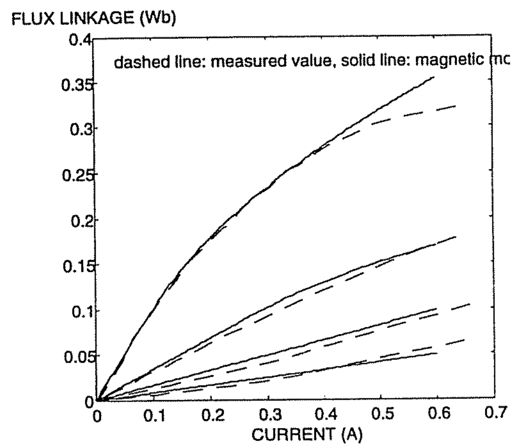

(a)

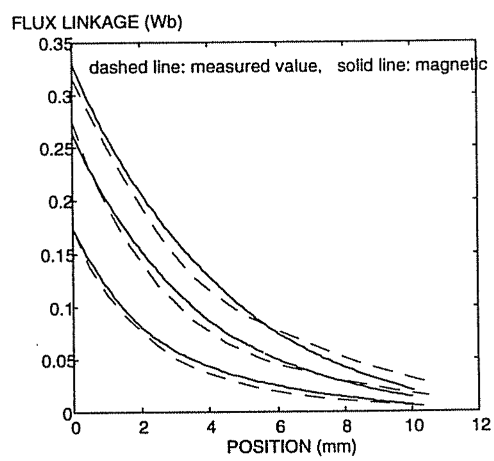

(b)

Figure 5. Comparison of the magnetic model with the actual measured values: (a) flux linkage vs. current, at x=0, 2.5, 5, & 7.5mm, (b) flux linkage vs. position, at i=0.2, 0.4, & 0.6A.

5. Modelling results

The six parameters mentioned in the earlier section were obtained by curve fitting equations 14 and 21 to the measured data. The flux linkage vs position and current from the six parameters vs measured values are indicated in figures 5(a) and 5(b) respectively. Close correspondence between the two sets are readily seen.

Computation of the force on the solenoid plunger is found from the co-energy (eqn 7). The computed and measured force data are shown together on the same graph in figure 6. Again, the predicted force is reasonably accurate except at the extreme positions of the solenoid. Such extreme positions may be avoided in actual operation without significant loss of operational range.

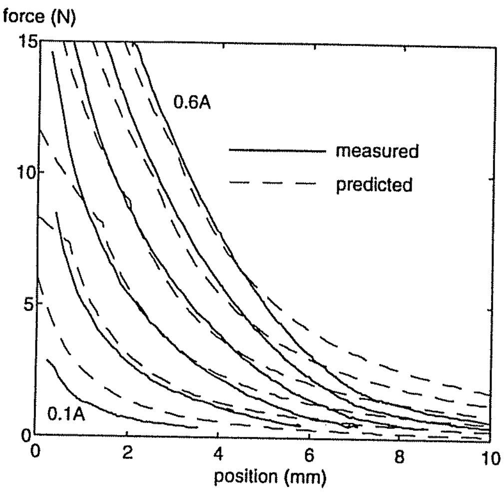

Figure 6. Comparison of predicted force with actual measurement.

Once the force is determined, the dynamics of the plunger is found from solving the electrical and mechanical equations (eqns. 8-10). Figures 7(a) and (b) compare the predicted and the actual dynamics of the solenoid when it is turned on.

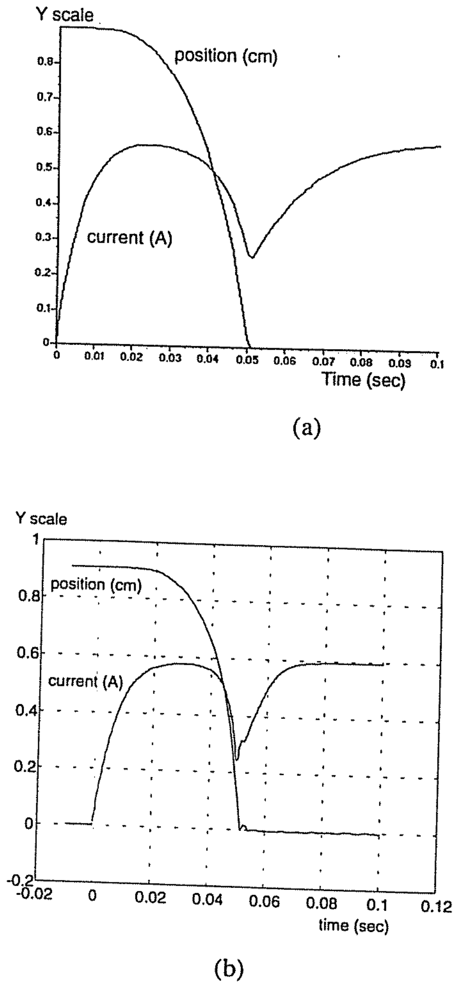

Figure 7. Dynamic response of the solenoid: (a) simulation result, and (b) actual measurement

6. Proportional Solenoid Development

Accurate modelling of the solenoid force and its dynamic response allows the analysis and design of a proportional solenoid. The control system of figure 8 is a closed loop positioning system with plunger position feedback which was also modelled and built experimentally. The results of the plunger position following in modelling and experimentation are shown in figures 9(a) and (b) respectively. It is clearly seen from these results that a proportional solenoid is feasible.

7. Conclusion

A non linear on/off solenoid has been modelled in terms of its magnetic and force characteristics and its dynamic response. The model is based on some simplifying assumptions which are appropriate to the solenoid's characteristics. The accurate modelling has allowed a proportional solenoid to be developed.

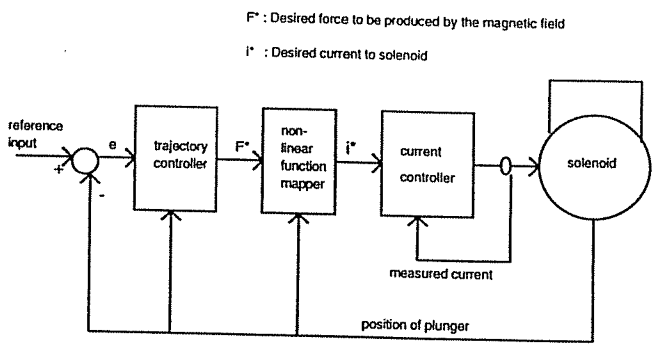

Figure 8. Block diagram of the control system.

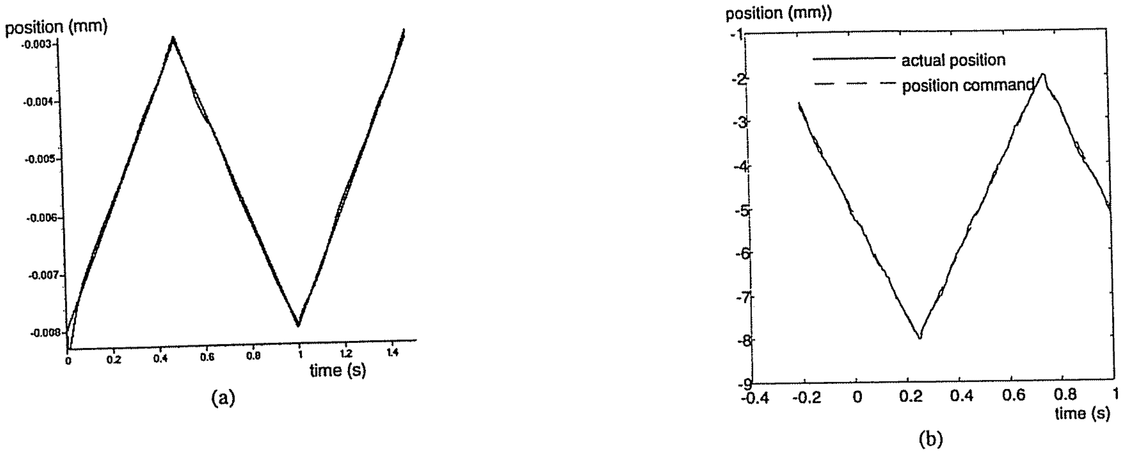

Figure 9. Simulation and actual results of position following.
(a) simulated ramp position following, (b) experimental.

References

[1] Lim K. W., Cheung N. C., M.F. Rahman, "Proportional control of a solenoid actuator," IEEE Industrial Electronics Society annual general meeting, Sept 1994, Bologna, Italy.

[2] Rahman M. F., Cheung N. C., Lim K. W., "Converting a switching solenoid into a proportional actuator," International Power Electronics Conference, IPEC'95, Yokohama, Japan.

[3] Filicori F., Bianco C. G. L., Tonielli A., "Modelling and control strategies for a variable reluctance direct drive motor," IEEE Trans. on Industrial Electronics, vol. 40, no. 1, pp105-115, February, 1993.

[4] Buja G. S, and Valla M. A., "Control characteristics of the SRM motor drives - Part I, operation in the linear region," IEEE Trans. on Industrial Electronics, vol. 38, no. 5, pp 313-321, October, 1991.

[5] Buja G. S., and Valla M. A., "Control characteristics of the SRM motor drives - Part II, operation in the saturated region," IEEE Trans. on Industrial Electronics, vol. 41, no. 3, pp 316-325, June, 1994.

[6] Goldenberg A. A., Laniado A., Kuzan P. and Zhou C., "Control of Switched Reluctance Motor Torque For Force Control Applications", IEEE Transactions on Industrial Electronics, Vol. 41, No. 4, pp 461-466, Aug 1994.

[7] Chai H. D., "A mathematical model for single stack step motors", IEEE Trans Power Apparatus ans Systems, PAS-94, pp1508-1517, 1975.

[8] Torrey D. A. and Lang J. H., "Modelling a non linear variable reluctance motor drive," IEE Proc. vol. 137, pt. B, no. 5, pp 314-326, Sept 1990.

[9] Manzer D. G., Varghese M., and Throp J. S., "Variable reluctance motor characterization," IEEE Trans. on Industrial Electronics, vol. 36, no. 1, pp 56-63, Feb 1989.

[10] Stephenson J. M. and Corda J., "Computation of torque and current in doubly salient reluctance motors from non linear magnetisation data", IEE Proc., pt. B, vol. 126, pp 393-396, 1979.

[11] Miller T. J. E. and McGilp M., "Non linear theory of the switched reluctance motor for rapid computer aided design," IEE Proc. vol 137, pt. B, no. 6, pp 337-346, Nov 1990.